JOURNAL OF AIRCRAFT
Vol. 34, No. 5, September–October 1997

Experimental Studies of a 70-Degree Delta Wing with Vortex Flaps

Kenichi Rinoie*
University of Tokyo, Tokyo 113, Japan
and
Toshimi Fujita,† Akihito Iwasaki,‡ and Hirotoshi Fujieda§
National Aerospace Laboratory, Tokyo 181, Japan

Force, surface pressure, and flowfield measurements were made on a 0.5-m root chord, 70-deg delta wing model with leading-edge vortex flaps at the National Aerospace Laboratory, Japan. The main objective of the experiment is to investigate the effect of the wing sweepback angle upon the vortex flap performance. Improvements in the lift/drag ratio were observed in a 70-deg delta wing by deflecting the tapered vortex flaps. Comparisons between the previously measured 60-deg delta wing results and the present results were made. The improvements in the lift/drag ratio of the 70-deg delta wing were attained over a narrower lift coefficient range than for the 60-deg delta wing. The results also showed that the maximum lift/drag ratio for the 70-deg delta wing is attained when the spanwise length of the separated region formed on the vortex flap surface almost coincides with the flap span.

Nomenclature

b = local span, m
C_D = drag coefficient
C_L = lift coefficient
C_m = pitching moment coefficient nondimensionalized using Cr and measured about $x/Cr = 0.67$
Cp = surface pressure coefficient, $(P - P_\infty)/q_\infty$
Cp_S = static pressure coefficient, $(P_S - P_\infty)/q_\infty$
Cr = wing centerline chord, m
L/D = lift/drag ratio
P = surface pressure, N/m^2
P_S = static pressure, N/m^2
P_∞ = freestream static pressure, N/m^2
q_∞ = freestream dynamic pressure, N/m^2
Re_{Cr} = Reynolds number based on the wing centerline chord
U_∞ = freestream velocity, m/s
x = chordwise coordinate measured from the apex of the delta wing, m
y = spanwise coordinate measured from the wing centerline, m
y_R = y coordinate of the deduced attachment point of the leading-edge separation vortex, m
z = coordinate normal to y and the freestream direction measured from the root chord line, m
α = wing angle of attack, deg
δ_f = vortex flap deflection angle measured normal to the hinge line, deg
Λ = model sweepback angle, deg

Presented as Paper 94-4.5.4 at the 19th International Council of the Aeronautical Sciences Congress (ICAS), Anaheim, CA, Sept. 18–23, 1994; and as Paper 96-2.10.2 at the 20th ICAS, Sorrento, Italy, Sept. 8–13, 1996; received March 23, 1997; revision received May 29, 1997; accepted for publication May 30, 1997.

*Associate Professor, Department of Aeronautics and Astronautics, 7-3-1 Hongo, Bunkyo-ku. Member AIAA.
†Senior Researcher, Advanced Aircraft Research Group, 6-13-1 Osawa, Mitaka.
‡Researcher, Advanced Aircraft Research Group.
§Senior Researcher, Advanced Aircraft Research Group.

Introduction

A DELTA wing is often used for high-speed aircraft, and it could be used for the next generation, high-speed civil transport aircraft. It is known that the aerodynamic characteristics of a delta wing at low speed are relatively poor. The leading-edge vortex flap (LEVF) is a leading-edge deflectable surface that can improve the aerodynamic efficiency of delta wings at low speeds.[1] A pair of leading-edge separation vortices are formed over the downward-deflected flap surfaces (Fig. 1). The vortices produce a forward-facing suction force, which reduces the drag and improves the L/D. References 2 and 3 give an overview of LEVF research. Rao[1] and Frink[4] tested a 74-deg delta wing with an LEVF. Marchman[5] tested 60- and 75-deg delta wings with a constant chord LEVF. Further investigations have been done for tabbed vortex flaps,[6] inverted vortex flaps,[7,8] and a double delta wing with the LEVF.[9] The effect of the delta wing thickness on the LEVF performance[10] and the effect of the LEVF on the vortex breakdown[8,11] have been investigated. Analytical studies using the free vortex sheet method were also done.[6,7,12] These investigations confirmed the benefit of the LEVF.

The first author has made experimental studies at various Reynolds numbers using two kinds of 60-deg delta wing models with sharp leading-edge and tapered LEVFs that have different cross sections.[13,14] One of the conclusions in Refs. 13 and 14 was that the highest L/D is achieved using a modest LEVF deflection angle that causes the flow to attach on the flap surface without any large separation. It was also shown that at higher lift coefficients, a modest improvement in L/D is obtained because of the suction force caused by the leading-edge separation vortex on the LEVF surface.[1] Most of the previous tests[1,4,5,10,11] were done using sweepback angles greater than 60 deg. References 5 and 15 tested a 60-deg delta wing, but with a constant chord LEVF. Therefore, it is of interest to know whether the conclusion in Refs. 13 and 14 is only applicable to a delta wing with a tapered LEVF, when $\Lambda = 60$ deg. It is also important to know whether changing the sweepback angle affects the flow around the tapered LEVF and the aerodynamics of the wing. Here, further wind-tunnel experiments have been made using a $\Lambda = 70$-deg delta wing model with a tapered LEVF in a 2×2 m low-speed wind tunnel at the National Aerospace Laboratory, Japan. The force and surface pressure measurements were made in the angle-of-attack

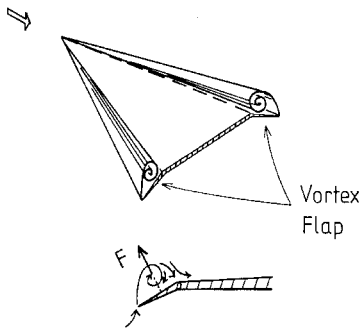

Fig. 1 Concept of vortex flap.[14]

range of −10 to +42 deg at a sideslip angle of 0 deg. The Reynolds number based on the wing centerline chord was 1×10^6. A five-hole pitot probe was used to investigate the structure of the leading-edge separation vortex formed over the LEVF surface. Comparisons between the previously measured 60-deg delta wing results and the present results are made to discuss the effect of the sweepback angle. The flow conditions giving the maximum L/D of the 60- and 70-deg delta wings with the LEVF are also discussed using these results.

Experimental Details

Figure 2 shows the model details. The model is a 70-deg flat-plate delta wing with no camber. The Cr is 0.5 m and the thickness is 0.015 m. The upper and lower surfaces are cut away so that the edges are sharp and have an apex angle of 8.6 deg at the two leading edges and 12.8 deg at the trailing edge, where the angle is measured in a plane normal to the edge. The model has the LEVF hinge lines running from the wing apex to 75% of the trailing-edge semispan station. Three rows of pressure tappings were located on the upper surface and one row was on the lower surface. Different flap deflections of $\delta_f = 0$ to 50 deg, in increments of 10 deg, were tested.

The experiments were made in a 2 × 2 m low-speed, closed working section, closed-return wind tunnel at the National Aerospace Laboratory in Japan. All tests were done at $U_\infty = 30$ m/s. The Re_{Cr} was 1×10^6. The freestream turbulence intensity of the tunnel is about 0.06%. The incidence range covered was from −10 to +40 deg. The model was mounted on a shielded strut with a tail sting. Lift, drag, and pitching moments were measured using the six-component pyramidal-type balance. To account for interference between the strut and the model, an interference correction using a dummy strut[16] was made in the angle-of-attack range from −10 to +10 deg. This range was limited because of the dummy strut geometry. Tunnel boundary corrections were applied to the measured data using the same method as in Refs. 13 and 14. The estimated overall accuracy of the lift, drag, and moment coefficients is ±1%, at 20:1 odds. As noted in Ref. 14, the accuracy at higher angles of attack reduces because of the higher tunnel wall interference. Surface pressure measurements were made using electronic scanner pressure sensors (ESP). The estimated overall accuracy of the pressure coefficient is ±2%, at 20:1 odds.

Flowfield measurements have been made using a five-hole pitot probe of 1.8 mm diameter. The probe was traversed in planes perpendicular to the freestream direction using the tunnel traversing-gear system. The position accuracy of the traversing-gear system is ±0.5 mm. The five-hole pitot pressure was measured using the ESP. The three-component velocities and the static pressure coefficient were obtained. The five-hole pitot probe has an accuracy, based on the calibration results, of less than ±4% error in absolute velocity and static pressure, and ±0.6-deg error in yaw and pitch angles. Because of the restriction of the five-hole pitot probe, the velocity vector that is inclined more than 30 deg to the freestream direction, or which is lower than 10 m/s, could not be evaluated. Measurements by the five-hole pitot probe at the vicinity of the wing surface are beyond the calibration range. However, the interference caused by the presence of the wall was not accounted for. The blockage effect of the five-hole pitot probe over the model has been checked by measuring the forces and surface pressure distributions, when the probe position against the model surface is changed. The results indicated that the effect of the probe is negligible if the angle of attack of the model is less than about 20 deg.

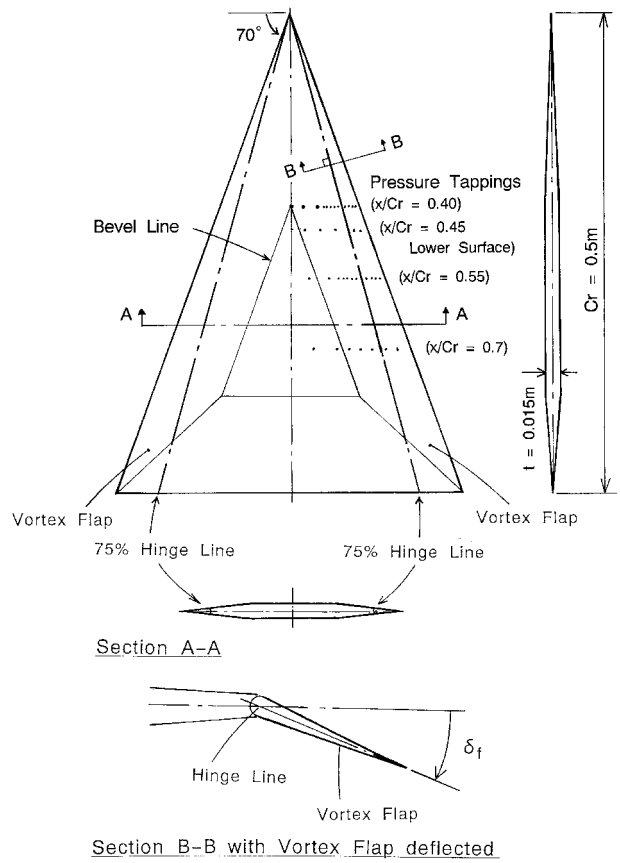

Fig. 2 70-deg delta wing model with LEVF.

Experimental Results

Three-Component Balance Measurements

The C_L vs α curves are shown in Fig. 3 for various δ_f. Results with strut interference correction are shown for $-10 < \alpha < 10$ deg, and results without strut interference correction for $\alpha > 10$ deg. Figure 3 shows that the C_L decreases as the LEVF is deflected downward. This trend is the same as that reported in Refs. 13 and 14. Comparisons with 70-deg flat-plate delta wing data in Ref. 17 are also shown in Fig. 3. In Ref. 17, measurements were made using a 70 deg, 0.10-in.-thick flat delta wing with beveled edges at a Reynolds number of 1×10^6. Excellent agreement with the present data for $\delta_f = 0$ deg is seen, except near $C_{L_{max}}$. The reason for the discrepancy near $C_{L_{max}}$ is discussed in the following section. The $C_D - \alpha$ curves (Fig. 4) show the C_D decreases for most of the positive α region, as δ_f increases.

Figure 5 shows L/D vs C_L. The results with strut interference correction are shown in the C_L range of $C_L \leq 0.4$, and results without the correction are shown in the C_L range of $C_L > 0.4$. A large L/D improvement for $\delta_f = 20$ and 30 deg is seen at about $C_L = 0.2-0.3$. This figure shows that the absolute maximum L/D of about 11.8 is observed at $\delta_f = 20$ deg, $\alpha = 5$ deg. However, the true peak in the L/D curve for the 30-deg flap case would lie between two of the illustrated optimum data points. Therefore, the absolute maximum L/D cannot be accurately evaluated from Fig. 5. It appears that the L/D im-

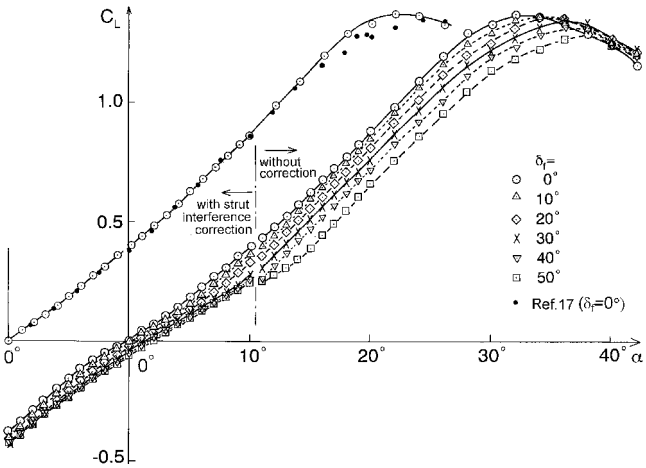

Fig. 3 Effect of LEVF on C_L vs α.

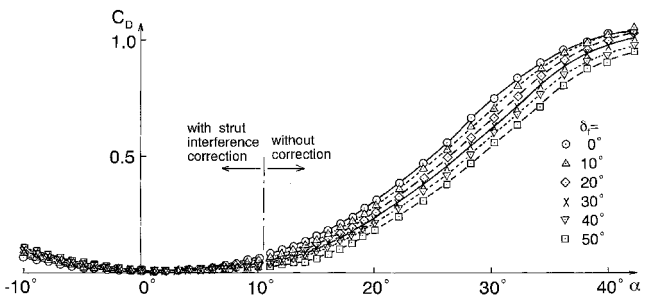

Fig. 4 Effect of LEVF on C_D vs α.

provement for the 20-deg flap case may be as great as that of the 30-deg case. In this context, the configuration at δ_f = 20 deg, α = 5 deg is hereafter referred to as the observed maximum *L/D* configuration. The results for all δ_f in the C_L range greater than about 0.5 show almost the same *L/D* distributions, which means that there is no benefit in using the LEVF for C_L > 0.5.

Figure 6 shows C_m vs C_L curves. The strut interference correction has not been included in Fig. 6. The LEVF has little effect on C_m. The aerodynamic center position measured from the $C_m - C_L$ slope is 0.58*Cr*, almost the same value as found for the 60-deg delta wing.[5]

Surface Pressure Distributions

Figure 7a shows surface pressure distributions at α = 5 deg for the upper surface at *x/Cr* = 0.55 and for the lower surface at *x/Cr* = 0.45, plotted against the semispanwise station *y*/(*b*/2). Results for flap deflection angles of δ_f = 0 to 50 deg are shown. The suction region is seen at *y*/(*b*/2) = 0.7–1.0 for the datum wing (δ_f = 0 deg). This suction region is thought to correspond to the leading-edge separation vortex.[14] The suction region is also seen at *y*/(*b*/2) = 0.8–1.0 for δ_f = 20 deg. The spanwise length of the suction region for δ_f = 20 deg is shorter than that for δ_f = 0 deg, and almost coincides with the vortex flap spanwise length. As the δ_f increases, the spanwise length of the suction region decreases. For δ_f = 50 deg, this suction region diminishes at the leading edge, but is seen inboard of the flap hinge line [*y*/(*b*/2) = 0.5–0.75]. This suggests that a separation region is formed inboard of the hinge line. The lower surface pressure distributions show very little change with δ_f.

Figure 7b shows surface pressure distributions on the upper surface at *x/Cr* = 0.55 for δ_f = 30 deg, when the angle of attack is changed from α = 0–18 deg. The suction region, which corresponds to the leading-edge separation vortex, grows as the angle of attack is increased. No suction region is

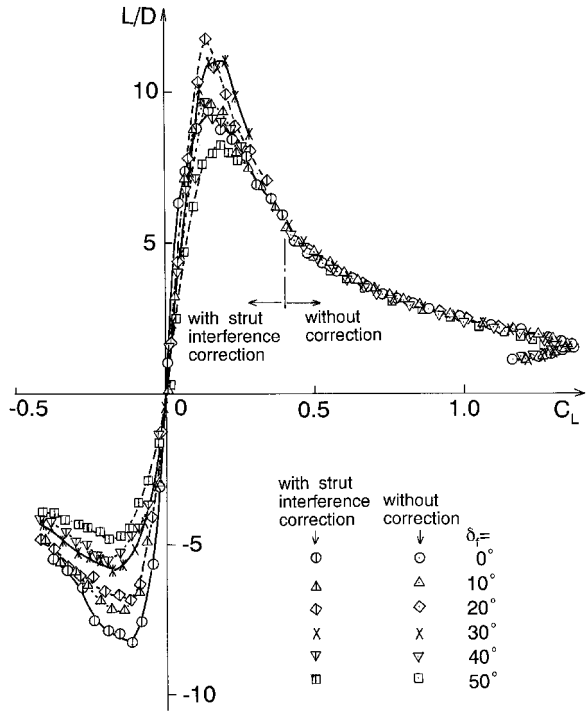

Fig. 5 Effect of LEVF on *L/D* vs C_L

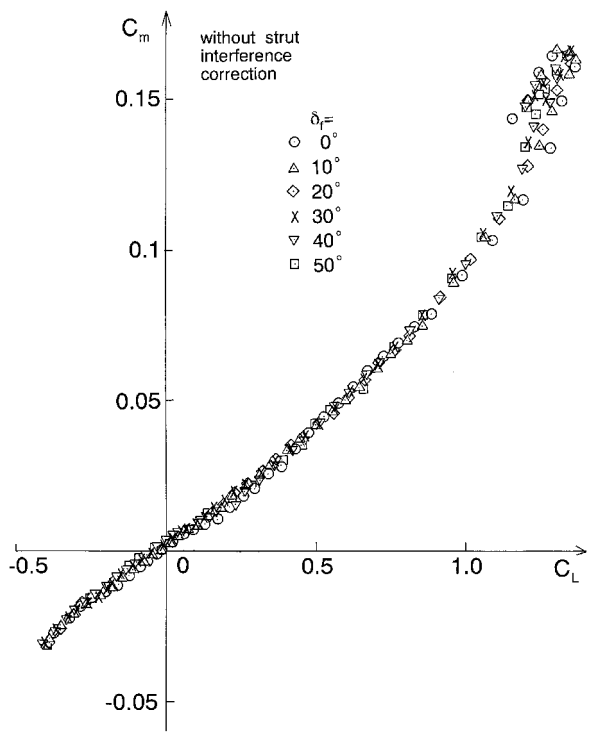

Fig. 6 Effect of LEVF on C_m vs *L/D*.

seen on the wing surface for α < 3 deg, which suggests that at these low angles the flow is attached over the flap.

Flowfield Measurements (Velocity Vectors)

Figure 8 shows the vectors of the velocity component, measured by the five-hole pitot probe, in a plane perpendicular to the freestream direction for δ_f = 0, 20, and 50 deg at α = 5 deg, *x/Cr* = 0.55. For δ_f = 0 deg (Fig. 8a), it is clearly seen that the leading-edge separation vortex is formed on the wing. The spanwise extent agrees well with that obtained from the surface pressure measurements in Fig. 7a. The x sign in Fig.

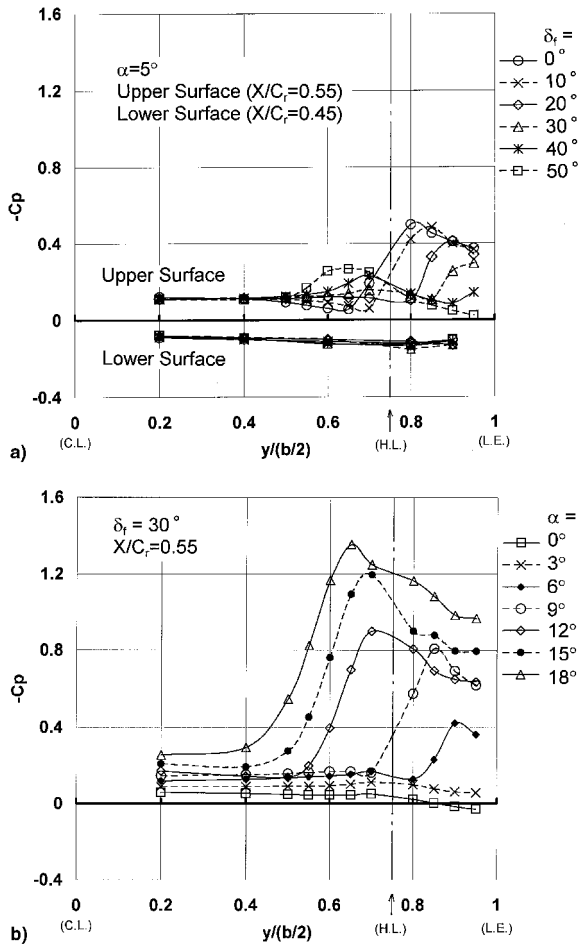

Fig. 7 Surface pressure distributions: a) α = 5 deg, *x/Cr* = 0.55, and b) δ_f = 30 deg, *x/Cr* = 0.55.

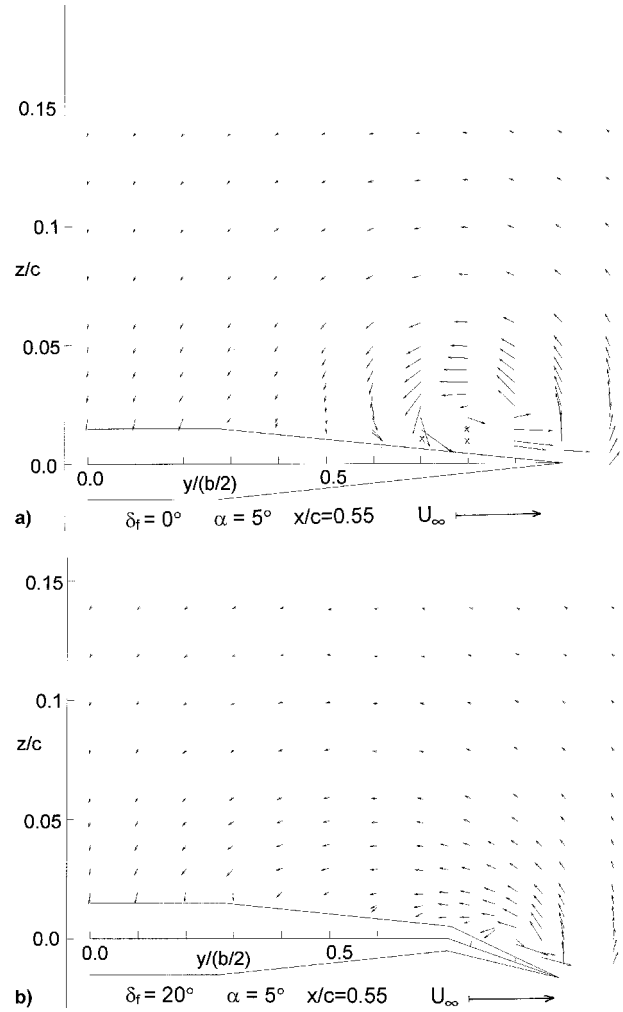

Fig. 8 Velocity vector components in the measuring plane at α = 5 deg, *x/Cr* = 0.55. δ_f = a) 0 and b) 20 deg.

8 denotes that the magnitude or the direction of velocity vector has exceeded the measurement accuracy, as described in the preceding section.

Figure 8b shows the velocity vector distributions for δ_f = 20 deg, when the observed maximum *L/D* is obtained. It is seen that a leading-edge separation vortex is formed and extends over nearly all the vortex flap. This again agrees with the indications from the pressure measurements (Fig. 7a).

Flowfield Measurements (Pressures)

Figure 9a shows results from flowfield measurements in the form of static pressure isobars for the no-flap deflection configuration (δ_f = 0 deg) at α = 5 deg. The surface pressure distributions for this case were shown in Fig. 7a, and the velocity vectors are shown in Fig. 8a.

Comparisons between the static pressure isobars in Fig. 9a and the velocity vectors in Fig. 8a show that the minimum Cp_S is attained at the core of the separation vortex. It is seen that the spanwise Cp_S distributions and the magnitude of Cp_S near the wing surface are similar to the surface pressure distributions in Fig. 7a. This confirms the upward suction force acting over the delta wing caused by the leading-edge separation vortex.

Figure 9b shows the Cp_S isobars for the 20-deg flap deflected at α = 5 deg. The leading-edge separation vortex is formed on the vortex flap surface as shown in Fig. 8b. The separation vortex formed on the vortex flap surface in Fig. 9b is much smaller and weaker than the separation vortex on the plain delta wing at the same angle of attack in Fig. 9a. However, results in Fig. 9 show similar isobar distributions for Cp_S. This indicates that the separation vortex formed on the vortex flap shows the same characteristics as those of the leading-edge separation vortex formed on a plain delta wing. Figure 9b shows that the minimum static pressure is attained at the core position of the separation vortex. This supports the idea of Rao[1] for a slender delta wing that the upward suction force acts on the vortex flap surface, the drag force acting on the wing decreases, and the *L/D* is consequently increased for the LEVF wing.

Comparisons Between the 60- and 70-Degree Delta Wings

The 60-deg delta wing model used in Ref. 14 and the present 70-deg delta wing model have similar planar shapes, though they do have different cross sections. The 60-deg delta wing model used in Ref. 14 has a symmetrical, smooth convex cross section. The present 70-deg delta wing model has a sharp beveled-edge flat-plate section. Measurements were made at different Reynolds numbers of $Re_{Cr} = 2 \times 10^6$ (Λ = 60 deg) and $Re_{Cr} = 1 \times 10^6$ (Λ = 70 deg). However, according to Refs. 18 and 19, it is known that the aerodynamic characteristics of sharp leading-edge delta wings and the behavior of the leading-edge separation vortex are not much affected by differences in either the model cross section or in the Reynolds number. It was also shown in Ref. 19 that the location of vortex-bursting that is observed at α > 25 deg for the Λ = 70-deg delta wing is significantly influenced by the model cross section, Reynolds number, and tunnel blockage. This explains the discrepancy in Fig. 3 between the present results and the data from Ref. 17 at angles of attack higher than about 24 deg. However, because this paper is mainly concerned with angles of attack when there is no vortex breakdown, it was concluded

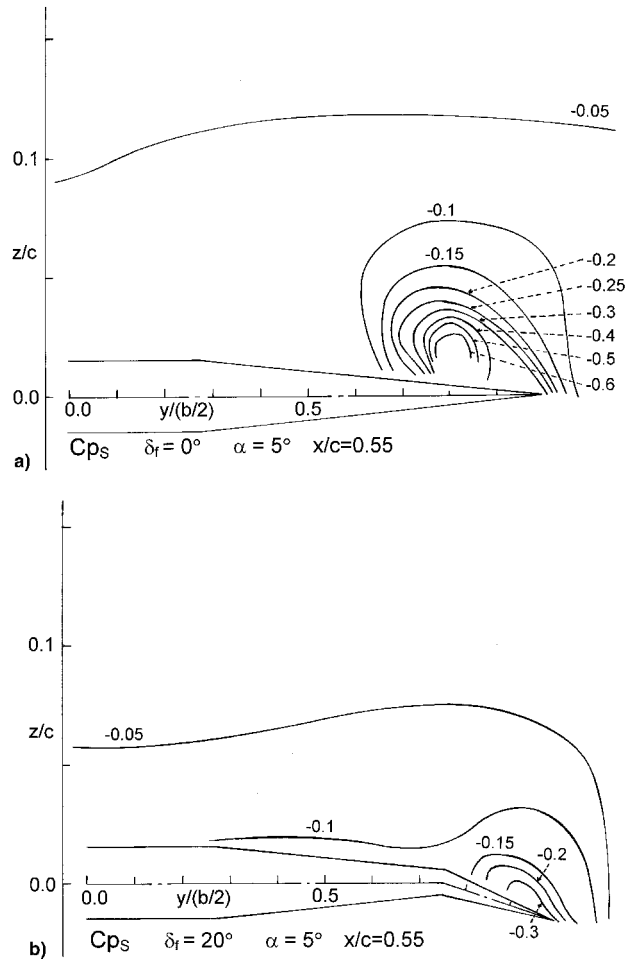

Fig. 9 Static pressure isobars at α = 5 deg. δ_f = a) 0 and b) 20 deg.

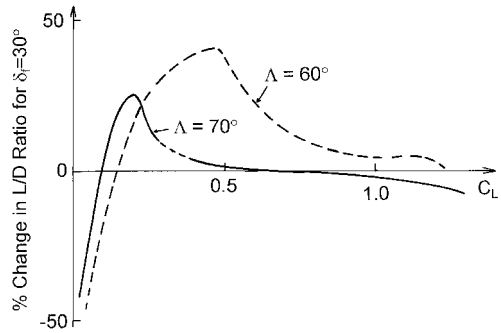

Fig. 10 Effect of LEVF on *L/D* improvements.

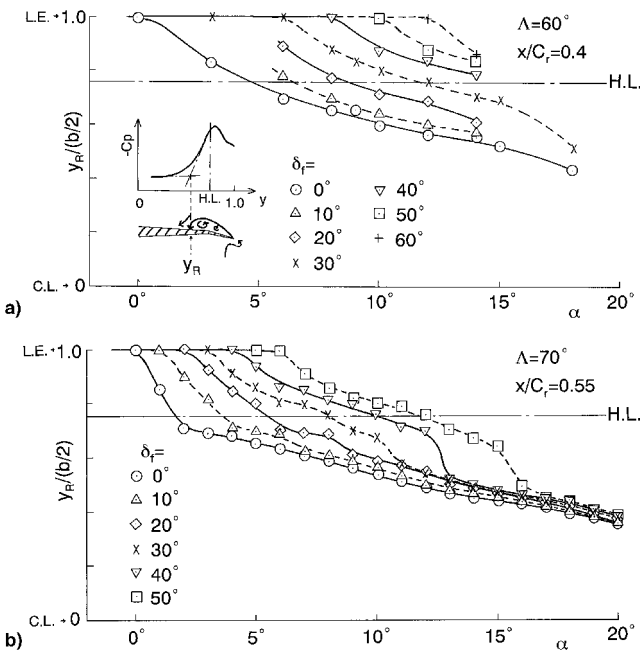

Fig. 11 Spanwise length of the leading-edge separation vortex vs α. Λ = a) 60 and b) 70 deg.

that the effect of the sweepback angle upon the LEVF characteristics could be investigated by comparing the present results with those of Ref. 14. In this section, the geometrical angle of attack as measured from the tunnel centerline without any tunnel wall correction is used.

L/D

To visualize the LEVF deflection effects on *L/D* more clearly, the percentage increase in *L/D* for δ_f = 30 deg is plotted against C_L in Fig. 10. This shows that the *L/D* is increased above that of the datum wing for C_L values between 0.15–1.2 for the 60-deg delta wing, and only between 0.1–0.5 for the 70-deg delta wing. The greatest percentage improvement is about 40% at a C_L of 0.45 for the 60-deg delta wing and about 26% at a C_L of 0.2 for the 70-deg delta wing. The C_L range in which the *L/D* is improved for the 70-deg delta wing is narrower than that for the 60-deg delta wing. Experiments for the 50-deg delta wing with the LEVF[20] showed similar results to those for the 60-deg delta wing, that the *L/D* is increased above that of the datum wing for C_L values between 0.15–0.8 for δ_f = 20 deg. A projected area of the vortex flap at the right angle to the flow direction goes down as the sweepback angle of the wing increases. Decrease in the projected area reduces the flap efficiency. This might be the reason for the difference between two delta wings in Fig. 10.

Spanwise Length of Leading-Edge Separation Vortex

Figure 11 shows the spanwise length of the leading-edge separation vortex region vs α at different δ_f for the 60- and 70-deg delta wings. The approximate attachment point of the leading-edge separation vortex as defined graphically from the surface pressure measurements in Fig. 11a is used. The spanwise coordinate y_R, measured from the wing centerline, is plotted in Fig.11 as an approximate attachment point of the vortex. The *Cp* results at *x/Cr* = 0.4 for the 60-deg delta wing, and *Cp* at *x/Cr* = 0.55 for the 70-deg wing were used for Figure 11. The reattachment point observed in Fig. 8 and that estimated in Fig. 11 are in close agreement. The distance between the attachment point and the leading edge [$y_R/(b/2)$ = 1.0] indicates the spanwise length of the leading-edge separation vortex region. When the attachment point coincides with the leading-edge position in Fig. 11, the flow is attached and the leading-edge separation vortex has not yet formed on the wing surface at these angles of attack. Comparisons between Figs. 11a and 11b show that as α is increased, the leading-edge separation vortex on the 70-deg delta wing begins to form at a smaller angle of attack than for the 60-deg delta wing. The separation occurs at a smaller angle of attack for the 70-deg delta wing than that for the 60-deg delta wing at the same δ_f. This is because the streamwise geometrical angle formed between the freestream and the flap surface of the 70-deg delta wing is larger than that of the 60-deg delta wing when compared at the same α and δ_f, because of the difference in the model sweepback angle.

Flow Around the LEVF at the Optimum *L/D*

According to the present results in Figs. 7a and 8b, a separation region is formed on the wing at the observed maximum *L/D* configuration at α = 5 deg, δ_f = 20 deg. The spanwise

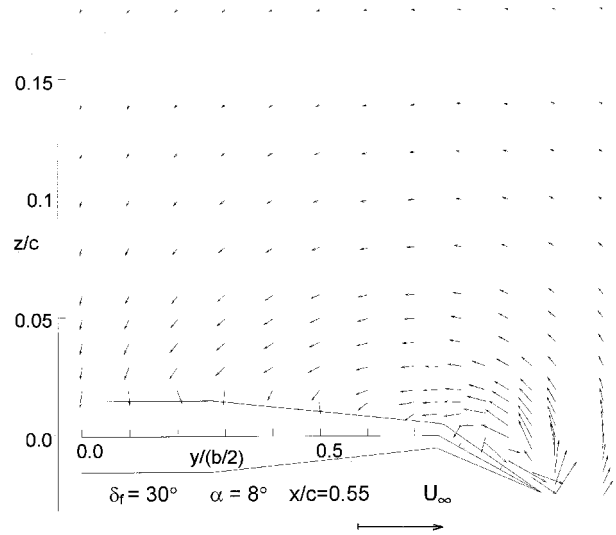

Fig. 12 Velocity vector components in the measuring plane at α = 8 deg, δ_f = 30 deg, and x/Cr = 0.55.

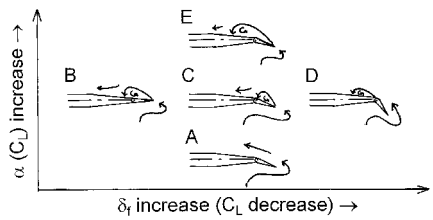

Fig. 13 Crossflow pattern sketches of LEVF.

length of this separation region almost coincides with the flap width. Because small errors in measuring C_D can have a large influence on the maximum L/D calculated, one other velocity vector distribution was measured at α = 8 deg, δ_f = 30 deg, when the wing attains the near maximum L/D of about 11.1 (Fig. 12). This figure shows that a leading-edge separation vortex is formed over the vortex flap. The flowfield pattern of Fig. 12 is almost identical to the results in Fig. 8b. Flowfield measurements for this model configuration were also made at x/Cr = 0.4 and 0.7. The results showed that the flow pattern of the separation vortex is the same for different chordwise stations. These results confirm that the maximum L/D ratio for the 70-deg delta wing is attained when the separated vortex is formed on the vortex flap and when its spanwise length coincides with the vortex flap span length.

Figure 13 summarizes the flow pattern sketches in the spanwise plane around the LEVF for different α and δ_f. These flow pattern sketches were deduced from the pressure measurements and the five-hole pitot probe measurements. At a constant flap deflection angle of δ_f, as α is increased (A $\rightarrow$ C $\rightarrow$ E in Fig. 13), a separated region increases in the spanwise extent. Conversely, at a reasonable constant α, increase in δ_f (B $\rightarrow$ C $\rightarrow$ D in Fig. 13) suppresses the separated region on the flap surface, and eventually the separation occurs from the knuckle point, i.e., the flap hinge line.

It was concluded in Ref. 14 that for the 60-deg delta wing, the highest value of L/D is achieved when the flow is attached over the LEVF surface, i.e., there is no separation over the flap. This conclusion was obtained for the 60-deg delta wing with tapered vortex flaps. However, if the vortex flap is sized differently and deflected properly, the separated flow in the vortex reattaches along the flap hinge line for the 60-deg delta wing that agrees with the original vortex flap concept.[1]

Conclusions

Force, surface pressure, and five-hole pitot probe measurements were made on a 70-deg delta wing with tapered LEVFs. These results were compared with previously measured results on a 60-deg delta wing.

1) Improvements in the L/D by deflecting the LEVF of a 70-deg delta wing were confirmed. Large improvements in the L/D are observed at lift coefficients between 0.2–0.3 for vortex flap deflections of 20 and 30 deg.

2) Separation vortices formed on a plain delta wing and on a vortex flap were clearly identified by the five-hole pitot probe.

3) Comparisons between the 60- and 70-deg delta wings show that improvements in the L/D of the 70-deg delta wing are attained over a narrower lift coefficient range than that for the 60-deg delta wing.

4) The present results confirmed that the maximum L/D for the 70-deg delta wing is attained, when a separated region is formed on the vortex flap and the spanwise length of this separated region almost coincides with the vortex flap width.

Acknowledgment

The authors express their gratitude to J. L. Stollery, College of Aeronautics, Cranfield University, United Kingdom, for his beneficial advice.

References

[1]Rao, D. M., "Leading-Edge Vortex-Flap Experiments on a 74 Deg. Delta Wing," NASA CR-159161, Nov. 1979.

[2]Lamar, J. E., and Campbell, J. F., "Vortex Flaps-Advanced Control Devices for Supercruise Fighters," *Aerospace America*, Vol. 22, Jan. 1984, pp. 95–99.

[3]Campbell, J. F., and Osborn, R. F., "Leading-Edge Vortex Research: Some Nonplanar Concepts and Current Challenges," *Vortex Flow Aerodynamics*, Vol. 1, NASA CP-2416, July 1986, pp. 31–63.

[4]Frink, N. T., "Subsonic Wind-Tunnel Measurements of a Slender Wing-Body Configuration Employing a Vortex Flap," NASA TM-89101, July 1987.

[5]Marchman, J. F., III, "Effectiveness of Leading-Edge Vortex Flaps on 60 and 75 Degree Delta Wings," *Journal of Aircraft*, Vol. 18, No. 4, 1981, pp. 280–286.

[6]Hoffler, K. D., and Rao, D. M., "An Investigation of the Tabbed Vortex Flap," *Journal of Aircraft*, Vol. 22, No. 6, 1985, pp. 490–497.

[7]Reddy, C. S., "Spanwise Pressure Distribution on Delta Wing with Leading-Edge Vortex Flap," *Journal of Aircraft*, Vol. 24, No. 3, 1987, pp. 222–224.

[8]Deng, Q., and Gursul, I., "Effect of Leading-Edge Flaps on Vortices and Vortex Breakdown," *Journal of Aircraft*, Vol. 33, No. 6, 1996, pp. 1079–1086.

[9]Traub, L. W., "Aerodynamic Characteristics of Vortex Flaps on a Double-Delta Planform," *Journal of Aircraft*, Vol. 32, No. 2, 1995, pp. 449, 450.

[10]Levin, D., and Seigner, A., "Experimental Investigation of Vortex Flaps on Thick Delta Wings," *Journal of Aircraft*, Vol. 31, No. 4, 1994, pp. 988–991.

[11]Erickson, G. E., "Water-Tunnel Studies of Leading-Edge Vortices," *Journal of Aircraft*, Vol. 19, No. 6, 1982, pp. 442–448.

[12]Reddy, C. S., "Effect of Leading-Edge Vortex Flaps on Aerodynamic Performance of Delta Wings," *Journal of Aircraft*, Vol. 18, No. 9, 1981, pp. 796–798.

[13]Rinoie, K., "Experiments on a 60° Delta Wing with Vortex Flaps and Vortex Plates," *Aeronautical Journal*, Vol. 97, No. 961, 1993, pp. 33–38.

[14]Rinoie, K., and Stollery, J. L., "Experimental Studies of Vortex Flaps and Vortex Plates," *Journal of Aircraft*, Vol. 31, No. 2, 1994, pp. 322–329.

[15]Rao, D. M., "An Exploratory Study of Area-Efficient Vortex Flap Concepts," *Journal of Aircraft*, Vol. 20, No. 12, 1983, pp. 1062–1067.

[16]Rae, W. H., Jr., and Pope, A., *Low Speed Wind Tunnel Testing*, 2nd ed., Wiley, New York, 1984, pp. 204–213.

[17]Wentz, W. H., Jr., and Kohlman, D. L., "Vortex Breakdown on Slender Sharp-Edged Wings," *Journal of Aircraft*, Vol. 8, No. 3, 1971, pp. 156–161.

[18]Rom, J., *High Angle of Attack Aerodynamics*, Springer–Verlag, New York, 1991, pp. 15–21.

[19]Kegelman, J., and Roos, F., "Effects of Leading-Edge Shape and Vortex Burst on the Flowfield of a 70 Degree Sweep Delta-Wing," AIAA Paper 89-0086, Jan. 1989.

[20]Rinoie, K., "Studies of Vortex Flaps for Different Sweepback Angle Delta Wings," *Proceedings of CEAS European Forum on High Lift and Separation Control* (Bath, England, UK), The Royal Aeronautical Society, London, 1995, pp. 22.1–22.8.